

Continuum Linear Response in Coordinate Space Hartree-Fock-Bogoliubov Formalism for Collective Excitations in Drip-line Nuclei

Masayuki Matsuo

Graduate School of Science and Technology, Niigata University, Niigata 950-2181, Japan

(March 28, 2024)

We formulate a continuum linear response theory on the basis of the Hartree-Fock-Bogoliubov formalism in the coordinate space representation in order to describe low-lying and high-lying collective excitations which couple to one-particle and two-particle continuum states. Numerical analysis is done for the neutron drip-line nucleus ^{24}O . A low-lying collective mode that emerges above the continuum threshold with large neutron strength is analyzed. The collective state is sensitive to the density-dependence of the pairing. The present theory satisfies accurately the energy weighted sum rule. This is guaranteed by treating the pairing self-consistently both in the static HFB and in the dynamical linear response equation.

I. INTRODUCTION

Collective excitation in exotic unstable nuclei, especially in neutron-rich nuclei near the drip-line, is one of the most interesting nuclear structure issues. The presence of the neutron halo or skin structures, or more generally of loosely bound neutrons and the very shallow Fermi energy will modify characters of collective excitations known in stable nuclei. It is further interesting if new kinds of collective mode emerge. The linear response theory or the random phase approximation is one of the powerful tools to study such issues. Since the method itself is a general framework to describe normal modes of excitation built on a reference state given by mean-field approximations [1], it is advantageous to, rather than very light drip-line nuclei such as ^{11}Li , heavier systems which will be studied in future experiments. Previous works in this direction have analyzed the giant resonances and the threshold neutron strength in exotic nuclei with closed shell configurations [2,4] with use of the continuum linear response theory formulated in the coordinate space [5,6]. However, to explore more systematically nuclei with open shell configurations, the theory has to be extended so as to take into account the pairing correlation, which may play essential roles especially for low-lying collective excitations.

Indeed the pairing correlation is a key element in the study of nuclei near the drip-line [7,9]. A special feature of the pairing in drip-line nuclei is that the correlation takes place not only among bound orbits in the potential well but also in continuum states above the zero energy threshold. The Hartree-Fock-Bogoliubov (HFB) theory formulated in the coordinate space representation [7,8] has a great power in this respect since it allows one to treat properly the pairing in the continuum orbits, whereas the conventional BCS approximation is not suited for this purpose. The coordinate space HFB has been applied extensively and clarifying some aspects of pairing effects on the ground state properties including the halo and the skin [7,8,10,17]. Descriptions of deformed exotic nuclei are also under current developments [18,22]. The coordinate space HFB has been also used together with the relativistic mean-field models [23,25].

The shallow Fermi energy in drip-line nuclei makes the threshold for particle continuum very low. It is therefore important to include effects of the continuum states in describing not only the ground state but also the excitation modes. Attempts have been made to describe both the pairing correlation and the continuum effects on collective states in the linear response formalism. These continuum quasiparticle linear response theories [26,29], however, rely on the conventional BCS approximation, which may not be very accurate near the drip-lines. On the other hand, an approach is proposed to build a quasiparticle random phase approximation (QRPA) with use of the canonical basis in the coordinate space HFB [30]. However, the continuum effect is not precisely accounted in this approach since the single-quasiparticle basis is discretized. Other QRPA models using the discrete BCS quasiparticle basis [31,33] have a similar problem.

In the present paper, we extend the approach of Ref. [5] and formulate a new continuum quasiparticle linear response theory that is fully based on the coordinate space HFB formalism, so that the theory can take into account coupling to the continuum configurations both in describing the pairing in the ground state and in description of collective excitations. A novel feature is that it includes, for the first time in the quasiparticle linear response formalism, the configurations where excited two quasiparticles are both occupying the continuum orbits above the threshold. We pay a special attention to consistency between the treatment of the pairing correlation in the static HFB and that in the linear response equation for

the collective excitations. This selfconsistency is quite important as we shall demonstrate in the following. We also discuss some basic features of pairing effects on collective excitations, taking as an example the quadrupole response in neutron rich oxygen isotopes including drip-line nucleus ^{24}O .

The sections xx2 and 3 are devoted to derivation of the basic equations of the linear response equations. Numerical results for oxygen isotopes are discussed in x4, and conclusions are drawn in x5.

II. TIME-DEPENDENT HARTREE-FOCK-BOGOLIUBOV EQUATION IN COORDINATE REPRESENTATION AND LINEARIZATION

A. TDHFB in coordinate space

The linear response theory or the random phase approximation can be formulated generally as a small amplitude limit of the time-dependent Hartree-Fock (TDHF) equation. Now in order to include the pairing correlations, we shall base our formulation on the time-dependent Hartree-Fock-Bogoliubov (TDHFB) theory. The TDHFB equations is often formulated with use of the discrete shell model single-particle basis and the Thouless representation [1,34], which however are not convenient to treat the continuum states. Thus we shall start our formulation with writing the basic equations of TDHFB in the coordinate space representation. It is an extension of the coordinate space HFB of Ref. [7] to time-dependent problems. We follow the notation of Ref. [7] in many aspects, while there are some differences since we do not impose the time-reversal symmetry assumed in Ref. [7].

The ground state of the system $|j_0\rangle$ in the HFB formalism is a vacuum of the Bogoliubov quasiparticles. We denote the annihilation and creation operators of the quasiparticles by $f_i; \quad g_i (i=1; \dots)$, which satisfy the vacuum condition $f_i |j_0\rangle = 0$. The nucleon operators (r) and ${}^y(r)$, where $\quad = 1=2$ denotes the spinor component, can be expanded by the quasiparticle operators as

$$(r) = \sum_i U_i(r) \quad i + V_i(r) \quad i^y = \sum_i '_{1i}(r) \quad i \quad '_{2i}(r\sim) \quad i^y; \quad (1a)$$

$${}^y(r) = \sum_i U_i(r) \quad i^y + V_i(r) \quad i = \sum_i '_{1i}(r) \quad i^y \quad '_{2i}(r\sim) \quad i; \quad (1b)$$

Here $'_{1i}(r)$ and $'_{2i}(r)$ are the single-quasiparticle wave functions that satisfy the coordinate space HFB equation [7] (see also the later description). We do not write explicitly the isospin degrees of freedom for simplicity although in actual applications the pairing correlation is taken into account separately for neutrons and protons. In the present paper we use functions $'_{1i}(r) = U_i(r)$ and $'_{2i}(r) = V_i(r\sim)$ instead of $U_i(r)$ and $V_i(r)$ for the convenience of notation whereas $U_i(r)$ and $V_i(r)$ correspond more directly to the $U;V$ matrices in the HFB formalism in the discrete shell model basis [1]. The symbol $'(r\sim)$ for a spinor function $'(r)$ denotes $'(r\sim) = (\quad 2)'$ $(r) = (\quad i \quad y')$ (r) . For the time-reversal convention, we employ $T'(r) = ' (r\sim) = (\quad i \quad y')$ (r) . These conventions are the same as in Ref. [7]. We also use a notation $'_1(r) = ' (r\sim)$ for the time-reversed function.

In a time dependent problem, the system is described by a TDHFB state vector $|j(t)\rangle$. We assume that at the initial time t_0 the nucleus is in the ground state, i.e. $|j(t=t_0)\rangle = |j_0\rangle$. Time evolution of the TDHFB state vector $|j(t)\rangle$ is governed by the time-dependent Schrodinger equation

$$i\hbar \frac{\partial}{\partial t} |j(t)\rangle = \hat{h}(t) |j(t)\rangle \quad (2)$$

with the time-dependent mean-field Hamiltonian $\hat{h}(t)$, which can be expressed generally as

$$\begin{aligned} \hat{h}(t) = & \int dr dr^0 \int^X h(r; r^0; t) \quad y(r) \quad (r^0) \\ & + \frac{1}{2} \int^Z \int^Z dr dr^0 \int^X \int^n \tilde{h}(r; r^0; t) \quad y(r) \quad y(r^0\sim) + \tilde{h}(r; r^0; t) \quad (r^0\sim) \quad (r) \\ & \int^Z dr \int^X y(r) \quad (r); \end{aligned} \quad (3)$$

where the second and the third terms represent the pair potential, and μ is the chemical potential or the Fermi energy. There are symmetry properties $h(r; r^0_0; t) = h(r^0_0; r; t)$ and $h(r; r^0_0; t) = h(r^0_{\sim 0}; r_{\sim}; t)$, which stem from the hermiticity of $\hat{h}(t)$ and the anti-commutation relation of the nucleon operators.

Using the unitary operator $\hat{U}(t)$ that describes the time evolution of $j(t)i$ by $j(t)i = \hat{U}(t)j_0i$, the nucleon operators in the Heisenberg representation $Y(r, t) = \hat{U}^\dagger(t)Y(r)\hat{U}(t)$ and $\tilde{Y}(r, t) = \hat{U}^\dagger(t)\tilde{Y}(r)\hat{U}(t)$ are introduced. They also have expansion in terms of the complete single-quasiparticle basis, given by

$$Y(r, t) = \sum_i \left(Y_{1,i}(r, t) a_i + Y_{2,i}(r_{\sim}, t) b_i^\dagger \right) \quad (4a)$$

$$\tilde{Y}(r, t) = \sum_i \left(\tilde{Y}_{1,i}(r, t) a_i^\dagger + \tilde{Y}_{2,i}(r_{\sim}, t) b_i \right) \quad (4b)$$

The single-quasiparticle wave functions $Y_{1,i}(r, t)$ and $Y_{2,i}(r, t)$ are now time-dependent, and they are at the initial time $t = t_0$ set to the ground state quasiparticle functions $Y_{1,i}(r)$ and $Y_{2,i}(r)$. The field equation of motion $i\hbar \frac{\partial}{\partial t} Y(r, t) = Y(r, t); \hat{h}_H(t)$ with $\hat{h}_H(t) = \hat{U}^\dagger(t)\hat{h}(t)\hat{U}(t)$ leads to the time-dependent Schrödinger equation for the single-quasiparticle wave functions $Y_{1,i}(r, t)$ and $Y_{2,i}(r, t)$, that is written as

$$i\hbar \frac{\partial}{\partial t} Y_{i}(r, t) = \int dr^0_0 H(r; r^0_0; t) Y_{i}(r^0_0, t); \quad (5)$$

where we have used a 2 × 2 matrix representation defined by

$$H(r; r^0_0; t) = \begin{pmatrix} h(r; r^0_0; t) & h(r, r^0) \\ h(r_{\sim}; r^0_{\sim}; t) & h(r_{\sim}; r^0_{\sim}; t) + h(r, r^0) \end{pmatrix}; \quad (6)$$

and

$$Y_i(r, t) = \begin{pmatrix} Y_{1,i}(r, t) \\ Y_{2,i}(r, t) \end{pmatrix}; \quad (7)$$

Note also that the same time-dependent single-quasiparticle equation (5) holds for $\bar{Y}_i(r, t)$ defined by

$$\bar{Y}_i(r, t) = \begin{pmatrix} Y_{2,i}(r_{\sim}, t) \\ Y_{1,i}(r_{\sim}, t) \end{pmatrix} = \begin{pmatrix} 0 & 1 \\ 1 & 0 \end{pmatrix} Y_i(r, t); \quad (8)$$

The bar implies the operation of $\begin{pmatrix} 0 & 1 \\ 1 & 0 \end{pmatrix}$. With these notations, Eq.(4) is written in a compact form

$$Y(r, t) = \sum_i Y_i(r, t) a_i + \sum_i \bar{Y}_i(r, t) b_i^\dagger; \quad (9)$$

A conjugate pair is formed by $Y_i(r, t)$ and $\bar{Y}_i(r, t)$. The orthonormality condition and the completeness for the single-quasiparticle states are expressed as

$$\int dr \sum_i Y_i(r, t) Y_j(r, t) = \int dr \sum_i \bar{Y}_i(r, t) \bar{Y}_j(r, t) = \delta_{ij}; \quad (10a)$$

$$\int dr \sum_i Y_i(r, t) \bar{Y}_j(r, t) = 0; \quad (10b)$$

$$\sum_i \left(Y_i(r, t) Y_i(r^0_0, t) + \bar{Y}_i(r, t) \bar{Y}_i(r^0_0, t) \right) = \begin{pmatrix} h(r, r^0) & 1 \\ 0 & 1 \end{pmatrix}; \quad (10c)$$

It is convenient to use the time-dependent density matrices in describing the evolution of the TDHFB state vector. We define the normal and the abnormal density (pair density) matrices by

$$\rho(r; r^0_0; t) = h(t)j^Y(r^0_0)(r)j(t)i = h_{0j}j^Y(r^0_0, t)(r)j_{0i}; \quad (11a)$$

$$\tilde{\rho}(r; r^0_0; t) = h(t)j(r^0_{\sim})(r)j(t)i = h_{0j}j(r^0_{\sim}, t)(r)j_{0i}; \quad (11b)$$

respectively. These definitions agree with those in Ref. [7] if the state vector time-independent $j(t)i = j_0i$ and the HFB ground state is time-even $T j_0i = j_0i$, although in this paper such assumption is not made. Also our definition of $h(r; r^0_0; t)$ and $\tilde{h}(r; r^0_0; t)$ reduces to those in Ref. [7] with the same conditions. The two density matrices are combined in a generalized density matrix R as

$$R(r; r^0_0; t) = \begin{pmatrix} h(t)j^y(r^0_0)(r)j(t)i & h(t)j(r^0_{\sim 0})(r)j(t)i \\ h(t)j^y(r^0_0)j(r_{\sim})j(t)i & h(t)j(r^0_{\sim 0})j(r_{\sim})j(t)i \end{pmatrix} = \begin{pmatrix} (r; r^0_0; t) & \sim(r; r^0_0; t) \\ \sim(r_{\sim}; r^0_{\sim 0}; t) & (r_{\sim}; r^0_{\sim 0}; t) \end{pmatrix} : \quad (12)$$

The generalized density matrix can also be expressed in terms of the time-dependent single-quasiparticle wave functions as

$$R(r; r^0_0; t) = \sum_i \begin{pmatrix} - & - \\ i & i \end{pmatrix} (r, t) \begin{pmatrix} - & - \\ i & i \end{pmatrix} (r^0_0, t) : \quad (13)$$

B. Linearization

Let us consider a TDHFB state vector $j(t)i$ which fluctuates around the HFB ground state j_0i under perturbation of an external field. The external perturbation induces also fluctuation in the selfconsistent mean-field. We now write the time-dependent mean-field Hamiltonian as $\hat{h}(t) = \hat{h}_0 + \hat{V}(t)$ where \hat{h}_0 denotes the static selfconsistent HFB mean-field Hamiltonian for the ground state while the fluctuating field $\hat{V}(t)$ contains both the external field $\hat{V}^{\text{ext}}(t)$ and the induced field $\hat{V}^{\text{ind}}(t)$. With presence of the pair correlation, the fluctuating field $\hat{V}(t)$ is a generalized one-body operator including pair creation and annihilation, which can be expressed as

$$\hat{V}(t) = \sum_r \sum_{r'} \int dr dr' \int dr^0 \int dr^0_0 v(r; r^0_0; t) j^y(r) j(r^0_0) + \frac{1}{2} \sum_r \int dr \int dr^0 \int dr^0_0 v(r; r^0_0; t) j^y(r) j^y(r^0_{\sim 0}) + \frac{1}{2} \sum_r \int dr \int dr^0 \int dr^0_0 v(r; r^0_0; t) j(r^0_{\sim 0}) j(r^0_0) ; \quad (14)$$

where we assume $\hat{V}(t)$ is hermitic. To describe response of the time-dependent single-quasiparticle wave function $\psi_i(r, t)$ to the perturbation, we expand it up to the linear order as

$$\psi_i(r, t) = e^{iE_i(t-t_0)=\hbar} (\psi_i(r) + \delta\psi_i(r, t)) : \quad (15)$$

Here $\psi_i(r)$ and E_i denote the quasiparticle functions and the quasiparticle excitation energy defined as a solution of the static HFB equation for the ground state,

$$H_0 \psi_i(r) = E_i \psi_i(r) ; \quad (16)$$

where H_0 is the 2×2 matrix representation of the static HFB mean-field Hamiltonian \hat{h}_0 .

An useful tool in describing the linear response is the single-particle Green function, which in our case is the single-quasiparticle Green function defined for the static HFB mean-field Hamiltonian \hat{h}_0 . Because of the pairing correlation, we need both the normal and abnormal Green functions

$$G_0(r, t; r^0, t^0) = \langle \psi_i(t, t^0) \psi_j^y(r, t); j^y(r^0, t^0) \rangle_{j_0i} ; \quad (17a)$$

$$F_0(r, t; r^0, t^0) = \langle \psi_i(t, t^0) \psi_j^y(r_{\sim}, t); j^y(r^0, t^0) \rangle_{j_0i} ; \quad (17b)$$

Here the nucleon operators $j^y(r, t) = \hat{U}_0^y(t) j^y(r) \hat{U}_0(t)$ and $\psi_j^y(r, t) = \hat{U}_0^y(t) \psi_j^y(r) \hat{U}_0(t)$ with $\hat{U}_0(t) = e^{i(t-t_0)\hat{h}_0=\hbar}$ evolve in time under the static HFB mean-field Hamiltonian \hat{h}_0 . More useful is the single-quasiparticle Green function in the 2×2 matrix representation [35,36] defined by

$$G_0(r, t; r^0, t^0) = \begin{pmatrix} \langle \psi_i(t, t^0) \psi_j^y(r, t); j^y(r^0, t^0) \rangle_{j_0i} & \langle \psi_i(t, t^0) \psi_j^y(r, t); j^y(r^0_{\sim}, t^0) \rangle_{j_0i} \\ \langle \psi_i(t, t^0) \psi_j^y(r_{\sim}, t); j^y(r^0, t^0) \rangle_{j_0i} & \langle \psi_i(t, t^0) \psi_j^y(r_{\sim}, t); j^y(r^0_{\sim}, t^0) \rangle_{j_0i} \end{pmatrix} : \quad (18)$$

The normal and abnormal Green functions G_0 and F_0 are contained in the 11 and 21 components, respectively. In the present paper we use the retarded functions in stead of the causal or Feynman functions. We call G_0 the HFB Green function. The Fourier transform of the HFB Green function $G_0(\mathbf{r}, \mathbf{r}^0; t, t^0)$ is given by $G_0(\mathbf{r}, \mathbf{r}^0; E + i\eta) = (E + i\eta - H_0)^{-1}$ where the infinitesimal constant $\eta > 0$ exhibits the causality. In actual numerical calculations, η is fixed to a small but finite number. Note that the HFB Green function can be constructed in different ways. If we adopt the spectral representation, it is expressed as

$$G_0(\mathbf{r}, \mathbf{r}^0; E) = \sum_i \frac{\psi_i(\mathbf{r}) \psi_i^*(\mathbf{r}^0)}{E - E_i} + \frac{\bar{\psi}_i(\mathbf{r}) \bar{\psi}_i^*(\mathbf{r}^0)}{E + E_i} \quad (19)$$

Another form which is useful to treat the continuum states is given in Ref. [35], which we utilize in the following.

The Fourier transform of the linear response χ_i of the single-quasiparticle wave function is now expressed as

$$\chi_i(\mathbf{r}, \mathbf{r}^0; \omega) = \int d\mathbf{r}^0 \int d\mathbf{r}^{\infty} G_0(\mathbf{r}, \mathbf{r}^0; \omega; \hbar\omega + i\eta + E_i) V(\mathbf{r}^0, \mathbf{r}^{\infty}; \omega) \chi_i(\mathbf{r}^{\infty}) \quad (20)$$

in terms of the HFB Green function. Here V is the matrix representation of the fluctuating field $\hat{V}(t)$, which is defined in the frequency domain by

$$V(\mathbf{r}, \mathbf{r}^0; \omega) = \begin{pmatrix} v(\mathbf{r}, \mathbf{r}^0; \omega) & \bar{v}(\mathbf{r}, \mathbf{r}^0; \omega) \\ \bar{v}(\mathbf{r}, \mathbf{r}^0; \omega) & v(\mathbf{r}, \mathbf{r}^0; \omega) \end{pmatrix} \quad (21)$$

For the conjugate wave function $\bar{\chi}_i$ holds the same equation except that the energy argument of the HFB Green function is replaced by $\hbar\omega + i\eta - E_i$.

Using the above results, the linear response in the density matrix $R(\omega) = R^{(0)} + R(\omega)$ is obtained as

$$R(\mathbf{r}, \mathbf{r}^0; \omega) = \int d\mathbf{r}_1 \int d\mathbf{r}_2 \sum_{i,j} G_0(\mathbf{r}, \mathbf{r}_1; E_i + \hbar\omega + i\eta) V(\mathbf{r}_1, \mathbf{r}_2; \omega) \bar{\chi}_i(\mathbf{r}_2, \mathbf{r}^0; \omega) + \bar{\chi}_i(\mathbf{r}, \mathbf{r}_1; \omega) V(\mathbf{r}_1, \mathbf{r}_2; \omega) G_0(\mathbf{r}_2, \mathbf{r}^0; E_i - \hbar\omega - i\eta) \quad (22)$$

Expectation value $A(t) = \langle \hat{A}(t) \rangle$ of a one-body operator

$$\hat{A} = \frac{1}{2} \int d\mathbf{r} \int d\mathbf{r}^0 \left[A_{11}(\mathbf{r}, \mathbf{r}^0) \psi(\mathbf{r}) \psi^*(\mathbf{r}^0) + A_{22}(\mathbf{r}, \mathbf{r}^0) \bar{\psi}(\mathbf{r}) \bar{\psi}^*(\mathbf{r}^0) + A_{12}(\mathbf{r}, \mathbf{r}^0) \psi(\mathbf{r}) \bar{\psi}^*(\mathbf{r}^0) + A_{21}(\mathbf{r}, \mathbf{r}^0) \bar{\psi}(\mathbf{r}) \psi^*(\mathbf{r}^0) \right] \quad (23)$$

is expressed in terms of the generalized density matrix as

$$A(t) = \int d\mathbf{r} \int d\mathbf{r}^0 \text{Tr} A(\mathbf{r}, \mathbf{r}^0) R(\mathbf{r}^0, \mathbf{r}; t) \quad (24)$$

with

$$A(\mathbf{r}, \mathbf{r}^0) = \begin{pmatrix} A_{11}(\mathbf{r}, \mathbf{r}^0) & A_{12}(\mathbf{r}, \mathbf{r}^0) \\ A_{21}(\mathbf{r}, \mathbf{r}^0) & A_{22}(\mathbf{r}, \mathbf{r}^0) \end{pmatrix} \quad (25)$$

where Tr denotes the trace with respect to the 2×2 matrix. Linear response of $A(t)$ in the Fourier representation is given by

$$A(\omega) = \int d\mathbf{r}_1 \int d\mathbf{r}_2 \int d\mathbf{r}_3 \int d\mathbf{r}_4 \sum_{i,j} \text{Tr} A(\mathbf{r}_1, \mathbf{r}_2) G_0(\mathbf{r}_2, \mathbf{r}_3; E_i + \hbar\omega + i\eta) V(\mathbf{r}_3, \mathbf{r}_4; \omega) \bar{\chi}_i(\mathbf{r}_4, \mathbf{r}_1) + \text{Tr} A(\mathbf{r}_1, \mathbf{r}_2) \bar{\chi}_i(\mathbf{r}_2, \mathbf{r}_3) V(\mathbf{r}_3, \mathbf{r}_4; \omega) G_0(\mathbf{r}_4, \mathbf{r}_1; E_i - \hbar\omega - i\eta) \quad (26)$$

in terms of the HFB Green function G_0 . Here A and B are 2×2 matrices which correspond to the normal and abnormal densities; $A = \begin{pmatrix} 2 & 0 \\ 0 & 0 \end{pmatrix}$; $\begin{pmatrix} 1 & 0 \\ 0 & 1 \end{pmatrix}$, and $\begin{pmatrix} 0 & 1 \\ 1 & 0 \end{pmatrix}$ for $\hat{\rho}(r) = \hat{\rho}(r)$; $\hat{\rho}_+(r)$, and $\hat{\rho}_-(r)$, respectively.

$B = \begin{pmatrix} 1 & 0 \\ 0 & 1 \end{pmatrix}$ for $\hat{\rho}(r) = \hat{\rho}(r)$, and B is the same as A for $\hat{\rho}(r) = \hat{\rho}_+(r)$; $\hat{\rho}_-(r)$.

If we insert Eq.(19) to the above equation, the unperturbed response function reduces to a spectral representation in a standard form

$$R_0(r; r^0; !) = \frac{1}{2} \sum_{ij} h_0 j^{\wedge}(r) \ddot{j} j i h i j j^{\wedge}(r^0) \ddot{j} i \frac{1}{h! + i E_i E_j} - h_0 j^{\wedge}(r^0) \ddot{j} j i h i j j^{\wedge}(r) \ddot{j} i \frac{1}{h! + i + E_i + E_j} ; \quad (35)$$

where

$$h i j j^{\wedge}(r) \ddot{j} i = \sum_i^X \rho_i^y(r) A_{ij}^{-y}(r); \quad (36a)$$

$$h_0 j^{\wedge}(r) \ddot{j} j i = \sum_j^X \rho_j^{-y}(r) A_{ji}^{-y}(r); \quad (36b)$$

This can also be derived directly from Eq.(33). This expression, however, is not convenient to treat the continuum states.

III. CORRELATED LINEAR RESPONSE WITH CONTINUUM STATES

A. Integral representation

If the nucleus is put in the space of infinite volume, the spectrum of HFB single-quasiparticle states become continuum for the quasiparticle excitation energy E which exceeds the one-particle separation energy $S_1 = \epsilon_j$ [7,35]. Accordingly, the single-quasiparticle HFB Green function G_0 also exhibits the continuum spectrum. Furthermore, the HFB Green function at the continuum energy is required to satisfy the boundary condition of outgoing wave in the exterior region of the nucleus [35], which is a suitable boundary condition for the continuum states. Let's us implement these features in the response functions.

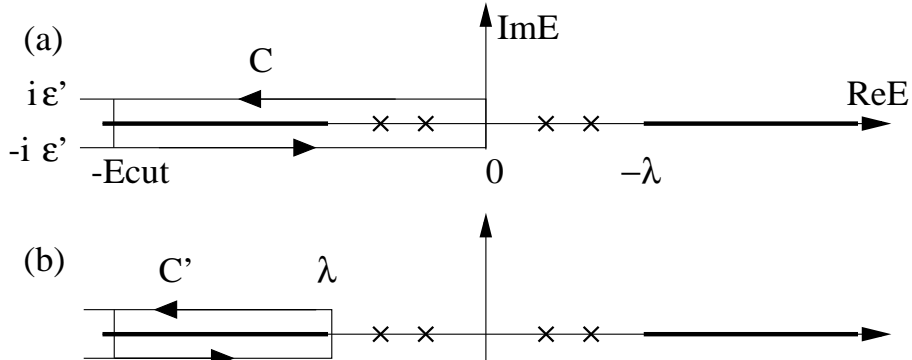


FIG. 1. Contours C and C' in the integral representation of the response function. The crosses represent the poles at $E = E_i$ corresponding to the bound quasiparticle states. The thick lines are the branch cuts.

This task is accomplished in two steps. Firstly, we handle the continuity of the HFB quasiparticle spectrum. For this purpose, we rewrite the summation over the HFB quasiparticles in Eq.(34) with use of an integral representation. Namely, a summation $\sum_i^P f(E_i) \rho_i^{-y}(r) \rho_i^{-y}(r)$ is replaced by a contour integral in the complex E plane as

$$\sum_i^X f(E_i) \rho_i^{-y}(r) \rho_i^{-y}(r) = \frac{1}{2\pi i} \int_C dE f(E) G_0(E); \quad (37)$$

in terms of the HFB Green function G_0 , Eq.(19), which has poles at $E = E_i$ on the negative energy axis. The contour has to be chosen so that it encloses these poles, and at the same time, it must avoid the poles associated with $G_0(E + h! + i)$ and $G_0(E - h! - i)$ that account for $G_0(E_i + h! + i)$ and $G_0(E_i - h! - i)$ in Eq.(34). A contour C satisfying this requirement is shown in Fig.1 (a), where the constant ϵ_0 must satisfy $\epsilon_0 > 0$. Consequently, the unperturbed response function is expressed as

$$R_0(r; r^0; !) = \frac{1}{4} \int_C \frac{dE}{i} \sum_{l,j} \text{Tr} \left[A G_0(r; r^0; E + h! + i) B G_0(r^0; r; E) + \text{Tr} \left[A G_0(r; r^0; E) B G_0(r^0; r; E - h! - i) \right] \right] \quad (38)$$

The contour is the same as those adopted in Refs. [35,17] except the condition for ϵ_0 .

For spherically symmetric systems, the partial wave expansion can be applied as

$$r(r) = Y_{ljm}(\hat{r}) \frac{1}{r} u_{lj}(r); \quad u_{lj}(r) = \begin{cases} u_{1,lj}(r) \\ u_{2,lj}(r) \end{cases}; \quad (39)$$

$$G_0(r; r^0; E) = \sum_{ljm} Y_{ljm}(\hat{r}) \frac{1}{r r^0} G_{0,lj}(r; r^0; E) Y_{ljm}(\hat{r}^0); \quad (40)$$

$$R_0(r; r^0; !) = \sum_{LM} Y_{LM}(\hat{r}) \frac{1}{r^2 r^0{}^2} R_{0,L}(r; r^0; !) Y_{LM}(\hat{r}^0); \quad (41)$$

with $Y_{ljm}(\hat{r})$ being the spin spherical harmonics. The unperturbed response function with the multipole L is then given by

$$R_{0,L}(r; r^0; !) = \frac{1}{4} \int_C \frac{dE}{i} \sum_{lj;l^0;j^0} \frac{h^{lj} j^0 k_Y L k_{lj} i^2}{2L + 1} \text{Tr} \left[A G_{0,l^0;j^0}(r; r^0; E + h! + i) B G_{0,lj}(r^0; r; E) + \text{Tr} \left[A G_{0,lj}(r; r^0; E) B G_{0,l^0;j^0}(r^0; r; E - h! - i) \right] \right] \quad (42)$$

If we treat separately the discrete and the continuum parts of the HFB spectrum, the following equivalent expression is obtained

$$R_{0,L}(r; r^0; !) = \frac{1}{2} \sum_{lj;l^0;j^0} \sum_n \frac{h^{lj} j^0 k_Y L k_{lj} i^2}{2L + 1} \sum_{n_{lj}}^{-T} \text{Tr} \left[A G_{0,l^0;j^0}(r; r^0; E_{n_{lj}} + h! + i) B_{n_{lj}}^-(r^0) + B_{n_{lj}}^-(r^0) G_{0,l^0;j^0}(r^0; r; E_{n_{lj}} - h! - i) A_{n_{lj}}^-(r^0) \right] + \frac{1}{4} \int_C \frac{dE}{i} \sum_{lj;l^0;j^0} \frac{h^{lj} j^0 k_Y L k_{lj} i^2}{2L + 1} \text{Tr} \left[A G_{0,l^0;j^0}(r; r^0; E + h! + i) B G_{0,lj}(r^0; r; E) + \text{Tr} \left[A G_{0,lj}(r; r^0; E) B G_{0,l^0;j^0}(r^0; r; E - h! - i) \right] \right] \quad (43)$$

where the summation \sum_n runs only over the bound single-quasiparticle states with discrete spectrum $E_{n_{lj}} < \epsilon_j$ while the contour C in the complex plane encloses only the continuum part, as shown in Fig.1 (b).

Having the integral representation of the response functions, we impose on the single-quasiparticle Green function the boundary condition of out-going wave in the exterior region. The HFB Green function satisfying this requirement is given in Ref. [35,17], which can be applied to spherically symmetric systems with local potential. Namely, the HFB Green function is constructed [35,17] as

$$G_{0,lj}(r; r^0; E) = \sum_{s;s^0=1;2}^X c_{lj}^{ss^0}(E) \begin{pmatrix} r \\ r^0 \end{pmatrix}_{lj}^{(+s)}(r; E) \begin{pmatrix} r^0 \\ r \end{pmatrix}_{lj}^{(s^0)T}(r^0; E) + \begin{pmatrix} r^0 \\ r \end{pmatrix}_{lj}^{(rs^0)}(r; E) \begin{pmatrix} r \\ r^0 \end{pmatrix}_{lj}^{(+s)T}(r^0; E); \quad (44)$$

Here $\begin{pmatrix} rs \\ lj \end{pmatrix}(r; E)$ ($s = 1;2$) are two independent solutions, regular at the origin $r = 0$, of the radial HFB equation

$$\frac{\hbar^2}{2m} \frac{d^2}{dr^2} + U_{lj}(r) \quad (r) \quad \frac{\hbar^2}{2m} \frac{d^2}{dr^2} + U_{lj}(r) + \quad (r) \quad \psi_{lj}(r;E) = E \psi_{lj}(r;E); \quad (45)$$

while $\psi_{lj}^{(+s)}(r;E)$ ($s = 1;2$) are two independent solutions that satisfy the boundary condition at $r \rightarrow 1$

$$\psi_{lj}^{(+1)}(r;E) \sim e^{ik_+(E)r} \quad ; \quad \psi_{lj}^{(+2)}(r;E) \sim e^{ik_-(E)r} \quad (46)$$

Here $k_{\pm}(E) = \sqrt{2m(E - \epsilon_{lj})}$ and the branch cuts are chosen so that $\text{Im} k_{\pm} > 0$ is satisfied. Thus the nucleons at $r \rightarrow 1$ is out-going for $E + i$ at the continuum energy $E > \epsilon_{lj}$ [35,17]. The coefficients $c_{lj}^{ss_0}(E)$ are expressed in terms of the Wronskians as

$$\begin{pmatrix} c_{lj}^{11} & c_{lj}^{12} \\ c_{lj}^{21} & c_{lj}^{22} \end{pmatrix} = \begin{pmatrix} w_{lj}(r_1;+1) & w_{lj}(r_1;+2) \\ w_{lj}(r_2;+1) & w_{lj}(r_2;+2) \end{pmatrix}^{-1} \quad (47)$$

with

$$w_{lj}(rs;+s_0) = \frac{\hbar^2}{2m} \left[\psi_{1;lj}^{(rs)}(r) \frac{d}{dr} \psi_{1;lj}^{(+s_0)}(r) - \psi_{1;lj}^{(+s_0)}(r) \frac{d}{dr} \psi_{1;lj}^{(rs)}(r) \right] + \left[\psi_{2;lj}^{(rs)}(r) \frac{d}{dr} \psi_{2;lj}^{(+s_0)}(r) - \psi_{2;lj}^{(+s_0)}(r) \frac{d}{dr} \psi_{2;lj}^{(rs)}(r) \right] \quad (48)$$

B. RPA response functions

Let us now describe linear response of the system by including correlation effects caused by the residual interactions among nucleons. The correlation brings about the induced field, which can be described as a fluctuating part of the selfconsistent mean-field associated with the TDHFB state vector $j(t)$. Generally, the expectation value of the total energy for $j(t)$ is a functional $E[R] = E[\rho; \tilde{\rho}; \tilde{\rho}]$ of the generalized density matrix R , or $\rho; \tilde{\rho}$, and $\tilde{\rho}$. The selfconsistent mean-fields h and \tilde{h} in Eq.(3) are then defined by a derivative of the functional with respect to the densities,

$$h(r; r^0; t) = \frac{\partial E}{\partial \rho(r^0; r; t)}; \quad (49a)$$

$$\tilde{h}(r; r^0; t) = 2 \frac{\partial E}{\partial \tilde{\rho}(r^0; r; t)}; \quad (49b)$$

If we assume zero-range effective interactions, the energy functional is expressed in terms of the local spin-independent densities $\rho(r;t) = \rho(r;t); \rho_{\pm}(r;t)$ and $\tilde{\rho}(r;t)$. In this case, the selfconsistent mean-field is expressed in the same form as Eq.(30) with the field functions given by

$$v(r;t) = \frac{\partial E}{\partial \rho(r;t)}; \quad (50)$$

Accordingly, the induced fields are

$$v^{ind}(r;t) = \sum_{gs} \frac{\partial v}{\partial \rho}(r) \rho(r;t) = \sum_{gs} \frac{\partial^2 E}{\partial \rho \partial \rho}(r) \rho(r;t); \quad (51)$$

Inserting $v = v^{ind} + v^{ext}$ to Eq.(32), we obtain the equation for the density linear response $\rho(r;t) = \rho(r;t); \rho_{\pm}(r;t)$, and $\tilde{\rho}(r;t)$, with the correlation effect taken into account. That is,

$$\rho(r;t) = \int dr \sum_{R_0} \rho(r^0;t) \sum_{gs} \frac{\partial v}{\partial \rho}(r^0) \rho(r^0;t) + v^{ext}(r^0;t); \quad (52)$$

This linear response equation is similar to the one in the continuum linear response theory for unpaired systems [5], but we here take into account the fluctuations in the pair densities. It is possible to write the above equation as

$$(\delta) = R_0(\delta) \frac{\partial v}{\partial} (\delta) + R_0(\delta) v^{\text{ext}}; \quad (53)$$

where the three kinds of density fluctuations are represented as a single extended vector $(\delta) = (\delta(r; \delta); \delta(r; \delta); \delta(r; \delta))^T$ with three components, and the same representation applies to the external fields v^{ext} . We consider both neutrons and protons in the actual application. Then the density response have six components (three for each isospin). The solution of the linear response equation is expressed as

$$(\delta) = \frac{1}{1 - R_0(\delta) \frac{\partial v}{\partial}} R_0(\delta) v^{\text{ext}} + R(\delta) v^{\text{ext}} \quad (54)$$

or

$$\delta(r; \delta) = \int_0^Z dr^0 \int^X R(\delta; r^0; \delta) v^{\text{ext}}(r^0); \quad (55)$$

where $R(\delta) = R(\delta; r^0; \delta)$ is the correlated response function. This is nothing but the response function in the random phase approximation (RPA).

The density response of the spherical system to an external field with the multipolarity L is given by

$$v^{\text{ext}}(r) = Y_{LM}(\hat{r}) v_L(r); \quad (56)$$

$$\delta(r; \delta) = Y_{LM}(\hat{r}) \frac{1}{r^2} \delta_L(r; \delta); \quad (57)$$

and the linear response equation

$$\delta_L(r; \delta) = \int_0^Z dr^0 R_{0,L}(\delta; r^0; \delta) \frac{\partial v}{\partial}(r^0) \frac{1}{r^2} \delta_L(r^0; \delta) + v_L(r^0; \delta) : \quad (58)$$

This equation can be solved numerically with use of the mesh representation of the radial coordinate in a way similar to Ref. [5]. The strength function for the response to the external field is expressed by means of the RPA response function as

$$\begin{aligned} S(n!) &= \sum^X j_n \hat{j}^{\delta} \delta^{\text{ext}} j_n \hat{j}^2 (n! - n!_k) \\ &= \frac{1}{-Im} \int_0^Z \int^Z dr dr^0 \int^X R_L(\delta; r^0; \delta) v_L(r) v_L(r^0) = \frac{1}{-Im} \int_0^Z dr \int^X v_L(r) \delta_L(r; \delta); \end{aligned} \quad (59)$$

Let us discuss characteristic features of our linear response theory by comparing with other approaches. Firstly, the present formalism includes the continuum quasiparticle states wherever they appear. Previous continuum QRPA's (or the continuum quasiparticle linear response theories) [26-29] adopt approximations that take into account the continuum boundary condition only for the normal Green function $G_0(E)$, but not for the abnormal Green function $F_0(E)$, while we have treated the single-quasiparticle HFB Green function exactly by using the construction by Belyaev et al. [35]. We also emphasize that the present theory includes the configurations where two nucleons are both in the continuum states. Since the HFB single-quasiparticle spectrum is made of the discrete bound orbits and the continuum unbound states, two-quasiparticle states are classified in three groups. The first is the one where both quasiparticles occupy two discrete bound states. The second is where one quasiparticle is in a bound state with discrete excitation energy E_i while the second quasiparticle occupy the continuum unbound states whose excitation energy E exceeds j_j . These one-particle continuum states emerge above a threshold excitation energy $E_{\text{th},1} = m + E_i + j_j$ where $m + E_i$ is the minimum quasiparticle excitation energy. In the unpaired limit, this threshold energy becomes identical to the excitation energy $\epsilon_{n,\text{last}}$ of nucleon from the last occupied hole orbit to the zero-energy threshold. The last group of two-quasiparticle states is the one where both two quasiparticles occupy continuum unbound states. The threshold excitation energy for the two-particle continuum states is $E_{\text{th},2} = 2j_j$ i.e. it is

twice the one-particle separation energy S_1 . The present theory includes all the three groups as seen in Eq. (43), whereas the previous approaches include only the configurations where only one nucleon is in the continuum states. Escaping processes of one particle to the external region takes part in at the excitation energy $h! > E_{th,1}$ above the one-particle threshold, and consequently the strength functions show continuum spectra. At excitation energy $h! > E_{th,2}$ above the two-particle threshold, processes of two-particle escaping contribute. A related point is that the previous continuum QRPA's adopt the BCS approximation that has difficulty to describe the pairing in the continuum, whereas we have exploited the coordinate space HFB formalism to remove the shortcoming.

Secondly, the present theory takes into account the particle-particle correlations associated with fluctuations in the pair densities \tilde{q}_+ , and \tilde{q}_- , which always emerge in paired systems. In other words, the pairing residual interaction contributes to the linear response equation (58). This particle-particle correlation has been neglected in many continuum quasiparticle linear response theories or QRPA's. Even when it is included [26,27], its effect is not clarified. We emphasize that this contribution should be included to keep a self-consistency of the pairing correlation, and it indeed has important consequences. This point is discussed in detail in the next section.

Thirdly, the present theory reduces to the continuum linear response theory for unpaired systems [5] if the HFB ground state has the zero pairing potential. This is easily seen in Eq.(43), which, in the zero pairing limit, has only the discrete part consisting of the occupied hole orbits n_1j . Note also that only the 11 component (the normal Green function G_0) of G_0 contributes to the response function for the density operator $\hat{\rho}(r)$. In this sense, the present theory is an extension of Ref. [5] to paired systems described by the coordinate space HFB.

IV. NUMERICAL ANALYSIS

We apply the above formalism to spin independent quadrupole excitations in open-shell oxygen isotopes near the neutron drip-line, where both the pairing correlation and the continuum effects may play important roles. In the following, we mainly discuss results for the drip-line nucleus ^{24}O . Since our purpose in this paper is to clarify basic characteristics of the theory, rather than to make a precise prediction, we adopt a simple model Hamiltonian which consists of a spherical Woods-Saxon potential and the residual two-body interactions.

As a pairing force we assume the density-dependent delta force [9,37]

$$V_{\text{pair}}(r; r^0) = \frac{1}{2} V_0 (1 - P)(1 - \tau_3)(\tau_3 = 0)(r = r^0); \quad (60)$$

where P is the spin exchange operator. The interaction strength depends on the position through the total nucleon density $\rho(r) = \rho_n(r) + \rho_p(r)$. With $\rho_0 = 0.16 \text{ fm}^{-3}$ (the saturation density), the pairing force is more effective at low-density nuclear surface than in the interior region. The density-dependent pairing force is widely adopted in the HFB calculations not only for unstable isotopes [8,14,18,19,22,23] but also for rapidly rotating deformed nuclei [37,38].

To obtain the ground state, we solve the radial HFB equation with the box boundary condition $\psi_i(r = R_{\text{max}}) = 0$ according to the procedure of Ref. [7], and determine selfconsistently the nucleon density $\rho_q(r)$ ($q = n, p$), the pair density $\tilde{q}_q(r)$ and the pairing potential $v_q(r) = V_0 (1 - \tau_3)(\tau_3 = 0) \tilde{q}_q(r)$. For the Woods-Saxon potential we adopt the standard parameter set [39,40]. We have used the radial mesh size $\Delta r = 0.2 \text{ fm}$, and the cut-off at $R_{\text{max}} = 20 \text{ fm}$. To evaluate the densities and the pairing potential, we include all the quasiparticle states whose excitation energy is below $E_{\text{max}} = 50 \text{ MeV}$ and with the orbital angular momentum $l_{\text{max}} \leq 7\hbar$. The pairing force strength V_0 is chosen $V_{0,p} = V_{0,n} = 520 \text{ fm}^{-3} \text{ MeV}$ so that the average neutron pairing gap $h_{n,i}$ in $^{18,20}\text{O}$ approximately agrees with the overall systematics $h_{n,i} \approx \frac{12}{A} \text{ MeV}$ [40]. Here we define the average gap by $h_{n,i} = \int dr \tilde{q}_n(r) \rho_n(r) / \int dr \tilde{q}_n(r)$, which corresponds to $h_{n,i_{uv}} = \int du v \tilde{q}_n(uv) / \int du v$ (denoting the canonical basis) adopted recently in the literature [41,38,22]. The calculated average neutron gap is $h_{n,i} = 2.74; 3.13; 3.30$, and 3.39 MeV for $^{18,20,22,24}\text{O}$, respectively. Note that the pairing gap increases as approaching the neutron drip-line line. For comparison, we use also the density-independent pairing interaction (the volume-type pairing), which is given by dropping the density-dependent term in Eq.(60). In this case, we use $V_0 = 240 \text{ fm}^{-3} \text{ MeV}$, $\tau_3 = 1$ so that the calculated average neutron gap $h_{n,i} = 2.70; 2.69; 2.26; 1.64 \text{ MeV}$ (for $^{18,20,22,24}\text{O}$) gives approximately the same value in $^{18,20}\text{O}$. The neutron pairing gap for the volume-type pairing decreases as increasing the neutron number,

especially at the drip-line nucleus ^{24}O . This trend is opposite to that for the density-dependent pairing, and consequently the calculated pairing correlation differs significantly for $^{22,24}\text{O}$ located near drip-lines even though the force parameter is adjusted in more stable $^{18,20}\text{O}$. Apparently, the density-dependent pairing force favors the pairing correlation in the low-density surface region which develops in nuclei near the drip-line. This is a characteristic feature of the density-dependent pairing [7,8,14].

The quadrupole response of the system is described by means of the linear response formalism presented in the previous section. As the residual interaction acting in the particle-particle channel, we use the same pairing interaction as that used for the static HFB calculation in order to keep the selfconsistency, which turns out very important in the following. For the particle-hole channel, we assume the Skyrme-type delta force

$$v_{ph}(r; r^0) = (t_0(1 + x_0 P) + t_3(1 + x_3 P))(r)(r^0); \quad (61)$$

where we adopt the same parameter as Ref. [5]; $t_0 = f(1100)\text{fm}^3\text{MeV}$, $t_3 = f(16000)\text{fm}^6\text{MeV}$, $x_0 = 0.5$ and $x_3 = 1$. Here the renormalization factor f is adjusted by imposing a selfconsistency [5] that the calculated static polarizability for the isoscalar dipole $\text{eld } D_{1M}^{IS} = \int r Y_{1M} + \int p r Y_{1M}$ becomes zero for each nucleus. The linear response equations are solved in the following way. The unperturbed response function is obtained by evaluating Eq.(42) where the contour integral is performed numerically with an energy step $jE_j = 16$. We use a small smoothing constant $\eta = 0.2\text{MeV}$, which corresponds to a smoothing with a Lorentzian function with FWHM of 0.4MeV . As for the HFB Green function we adopt the exact expression (44), and evaluate the radial functions (also the response functions) by using the mesh $r = 0.2\text{fm}$ and the cut-off radius $R_{max} = 20\text{fm}$. In evaluating Eq.(42), we introduce also the angular momentum cut-off $l_{max} = 7h$. These parameters are the same as in solving the static HFB calculation. The cut-off energy for the contour integral is $E_{cut} = 50\text{MeV}$, which is a natural choice since it is the same cut-off energy E_{max} for the static HFB. Because the value of E_{cut} is larger than the potential depth (measured from the Fermi energy), the contour integral can include all the hole orbits in the limiting case of the zero pairing potential. We thus guarantee that in the zero pairing limit the evaluated response function for the density operator becomes identical to the response function for unpaired systems [5]. The RPA response functions $R(r; r^0; h!)$ is obtained by solving Eq.(58), which is a 600×600 linear matrix equation in the radial mesh representation.

Figure 2 shows the strength functions calculated for the quadrupole excitation in ^{24}O . Here we show the strength function $S(h!) = dB(Q_{2;0_{gs}^+}; k) = d(h!) = \sum_{Mk} Q_{gs}^+ Q_{2M}^k i^2 (h! h!_k)$ for the neutron and proton quadrupole moments $Q_{2M}^n = \int r^2 Y_{2M}$ and $Q_{2M}^p = \int p r^2 Y_{2M}$, the isoscalar and isovector quadrupole moments $Q_{2M}^{IS} = Q_{2M}^n + Q_{2M}^p$, and $Q_{2M}^{IV} = Q_{2M}^n - Q_{2M}^p$ as a function of the excitation energy $h!$. Plotted here is the strength functions summed over the magnetic quantum number M so that their energy integral are equivalent to $B(Q_{2;0_{gs}^+}; 2^+)$. A noticeable feature seen in Fig.2 is presence of a sharp and intense peak around $h! = 5.0\text{MeV}$. There also exist a resonance peak around $h! = 17\text{MeV}$ with a width of

3MeV , and in addition a very broad distribution around $h! = 20 - 40\text{MeV}$. These two modes correspond to isoscalar (IS) and isovector (IV) giant quadrupole resonances (GQR) whereas they are not pure ISGQR nor IVGQR since a large admixture of isovector (isoscalar) strength is present in each resonance region of the isoscalar (isovector) modes.

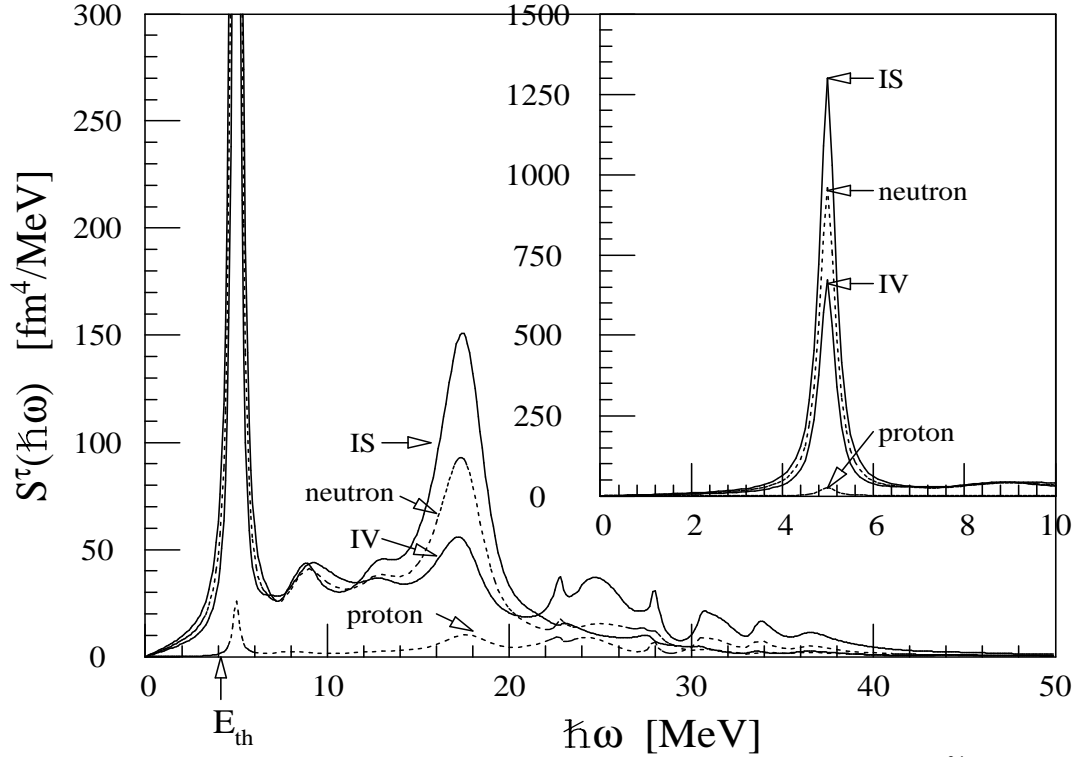


FIG. 2. The strength functions for the quadrupole moments Q_{2M} ($= IS; IV; n; p$) in ^{24}O with use of the density-dependent pairing force. The renormalization factor for the particle-hole residual interaction is $f = 0.632$. Solid and dotted curves represent those for $Q_{2M}^{IS}; Q_{2M}^{IV}$, and $Q_{2M}^n; Q_{2M}^p$, respectively. The inset shows a magnified part for the low excitation energy $h\omega < 10$ MeV. The threshold energy $E_{th,1} = E_{th,2} = 2j = 4.14$ MeV is indicated by an arrow.

The peak excitation energy of the low-lying mode is $h\omega = 5.0$ MeV. Since the threshold energies for one-neutron and two-neutron continuum states are, $E_{th,1} = E_{th,2} = 4.14$ MeV, the low-lying neutron quadrupole mode is embedded in the neutron continuum states. The FWHM width of this mode (45 keV) is almost the same as the smoothing width $2\gamma = 40$ keV, indicating that the mode has very small escaping width in spite of the coupling to the neutron continuum states.

The low-lying quadrupole mode at $h\omega = 5.0$ MeV is characterized by very large neutron strength. The isoscalar strength is also large, but the proton strength is small. The isovector strength is sizable but smaller than the neutron and isoscalar strengths because the small proton contribution is in phase with the neutrons. The integrated neutron strength $B(Q^{\pi 2})$ below $h\omega = 6.0$ MeV is 605 fm^4 whereas $B(E2) (= e^2 B(Q^{\pi 2}))$ is only $16.4 e^2 \text{ fm}^4$. Converting the strengths to the neutron/proton ratio M_n/M_p for the quadrupole transition amplitudes, it is evaluated as $M_n/M_p = 6:1$. The neutron character of this mode is apparent by comparing this value to a simple macroscopic estimate $M_n/M_p = N/Z = 2$. The low-lying mode exhausts approximately 20%, 10% and 19%, of the sum rule value for the isoscalar, isovector, and neutron quadrupole transition strength, respectively (See Eq.(62) and Fig. 6(a)). This ratio is much larger than a typical value for the low-lying isoscalar quadrupole mode (10%) [42]. On the contrary, the proton strength (i.e. the $B(E2)$ strength) is small, exhausting only 2% of the energy weighted sum rule. The strength of the low-lying neutron mode is continued to the neutron strength distribution in the interval ($h\omega = 6 - 15$ MeV) between the low-lying mode and the giant resonances, which corresponds to the so called threshold strength. However, the character of the low-lying neutron mode clearly differs from that of the threshold strength [2] since its large neutron strength of collective nature is generated by the residual interaction (see below). We note also that the HFB single-quasiparticle states have no discrete bound orbits, instead they are all continuum states or resonances. The low-lying neutron mode is a collective state made of continuum two-quasiparticle states.

We have also calculated the quadrupole strength functions for $^{18;20;22}O$. The peak energies of the low-lying mode is $h\omega = 4.2; 4.1; 4.5; 5.0$ MeV for $A = 18; 20; 22; 24$, respectively, which is 1-2 MeV higher than the experiments [32,43,46]. The calculated neutron strength ($B(Q^{\pi 2}) = 152; 295; 426; 605 \text{ fm}^4$ for $A = 18-24$) increases sharply with increasing the neutron number. On the contrary, the calculated $B(E2) = 15; 18; 17; 17 e^2 \text{ fm}^4$ ($A = 18 - 24$) stays almost constant. The calculation underestimates the experimental

B(E2) value [43,44,32,45] by a factor of 3-1.5 for $^{18;20}\text{O}$, but with reasonable agreement in ^{22}O . The calculated B(E2) values differs by a factor of 0.5-1.5 from the quasiparticle RPA calculation in Ref. [31,32]. The adopted model Hamiltonian, especially the Woods-Saxon potential, should be improved to make more quantitative comparison, e.g. by using more realistic Skyrme interaction both for the Hartree-Fock potential and for the particle-hole interactions. Leaving such improvements for a future investigation, we in the following focus on basic aspects of the present theory.

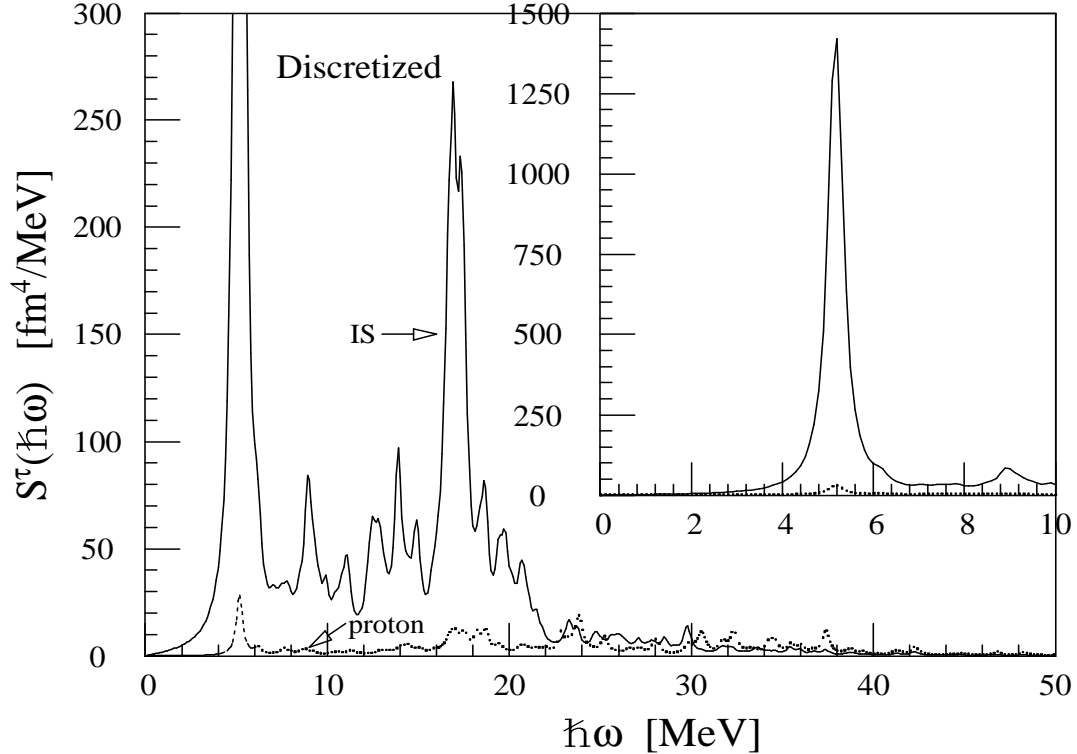


FIG. 3. The strength functions for the isoscalar and proton quadrupole moments Q_{2M}^{IS} and Q_{2M}^P in ^{24}O with use of the density-dependent pairing force, calculated with the discretized continuum states (see text). The renormalization factor for the particle-hole residual interaction is $f = 0.702$. Solid and dotted curves represent those for Q_{2M}^{IS} and Q_{2M}^P , respectively.

The present theory takes into account the one- and two-particle continuum states without making any discretization method or bound state approximation. It is interesting in this respect to see difference between the results presented above and results that would have been obtained by using discretized continuum states. We show in Fig.3 the strength function obtained by using the discrete spectral representation Eq.(35) instead of Eq.(42). Here we solve discrete single-quasiparticle states with the box boundary condition $\psi_i(R_{max}) = 0$, and adopt all the quasiparticle states with the excitation energy E_i below the energy cut-off $E_{max} = 50$ MeV and the angular momentum cut-off $l_{max} = 7$, including the discretized states in the continuum region $E_i > j j$. The renormalization factor f is slightly changed in this approximate calculation in order to reproduce the zero energy dipole mode. With use of the discretized continuum approximation, the strength function consists only of discrete states (but smeared with the smearing width) even in the continuum region above the threshold. This causes spurious fluctuation, as seen in Fig.3. It is noted on the other hand that a gross profile of the strength distribution is described fairly well by the discretizing approximation. It can be expected that in the limit of large box size $R_{max} \rightarrow \infty$, the discretizing approximation would give the same results with the one obtained with the continuum linear response theory, whereas such limiting is practically very difficult. Note also that the strengths associated with the low-lying neutron mode at $h\omega \approx 5$ MeV are almost reproduced by the discretizing approximation. This is because the low-lying mode in the present model calculation is a very narrow resonance, for which a bound state approximation can be a reasonable approximation.

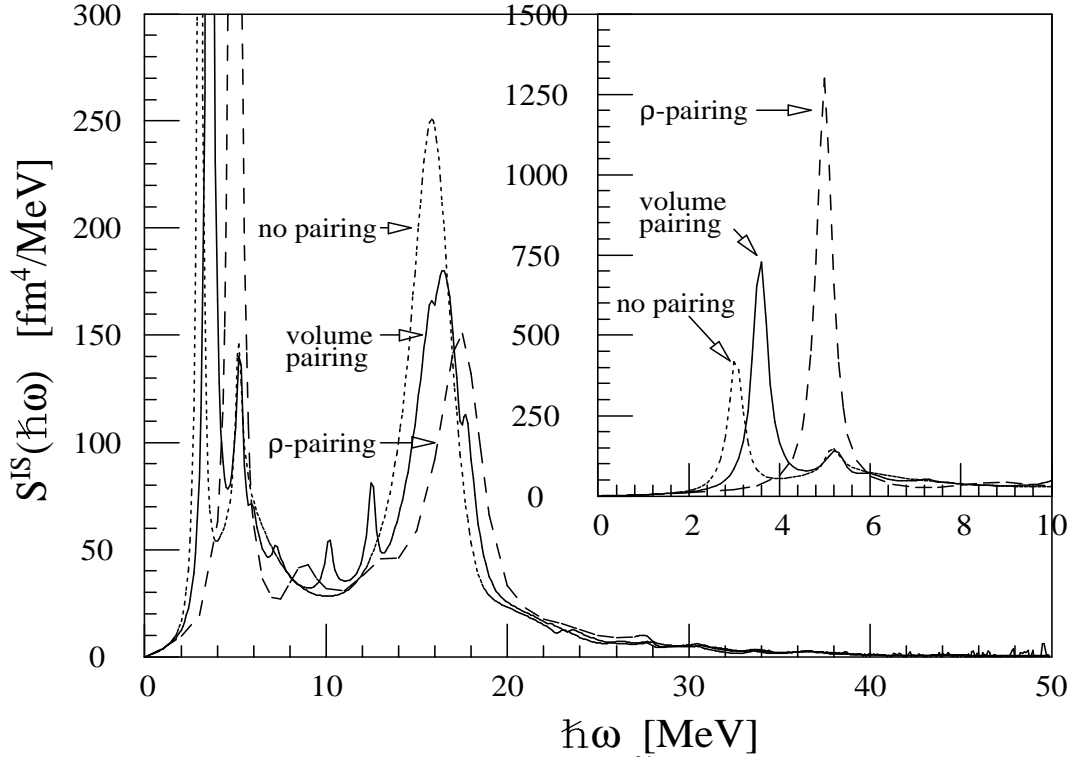


FIG. 4. Dependence of the quadrupole strength function in ^{24}O on the pairing interaction. Plotted are the strength functions for the isoscalar quadrupole moment Q_{2M}^{IS} for the density-dependent pairing (dashed curve), for the volume-type pairing (solid), and for the case where the pairing is neglected (dotted). See text for details. The renormalization factor for the particle-hole residual interaction is $f = 0.702$.

The pairing correlation play various important roles for the response. We show in Fig.4 the calculation without the pairing correlation (i.e. the pairing interaction is neglected both in the static HFB and the linear response equation). In this case, the quadrupole strength in the low-energy region becomes much smaller. The small peak at $\hbar\omega \approx 3.0$ MeV is not very collective, but it is basically non-collective neutron particle-hole transition $2s_{1/2} \rightarrow 1d_{3/2}$ with slight enhancement due to correlation. It is clearly seen that the pairing increases the collectivity of the low-lying neutron mode. The pairing effect on the low-lying isoscalar quadrupole mode in stable nuclei is well known [42]. Our result suggests a similar effect on the neutron mode, which is embedded in the continuum states in the case of drip-line nuclei.

We found further that the low-lying neutron mode is quite sensitive to the density-dependence of the pairing. Figure 4 shows also the result that is obtained with the density-independent volume-type pairing force in place of the density-dependent one Eq.(60). The neutron (and isoscalar) strength in the low-lying neutron mode obtained in this calculation is significantly smaller, i.e. it is about 50% of that with the density-dependent pairing. Using this sensitivity, one may be able to probe the density-dependence of the pairing. The difference between the density-dependent and the volume pairing is most significant in ^{24}O , but not very large in the other oxygen isotopes, which is in accordance with the behavior of the average neutron gap \hbar_{ni} discussed above. Fig. 4 shows that the pairing correlation influences also the strength distribution in the giant resonance region. It has an effect to reduce the strength in the high-lying modes. An apparent reason is that the low-lying neutron mode collects nearly 20% of the total energy weighted isoscalar and neutron sum S in the case of the surface pairing, and removes corresponding amount of strength from the giant resonance region because of the sum rule. The peak position and width (distribution profile) of GR's are also slightly affected by the pairing.

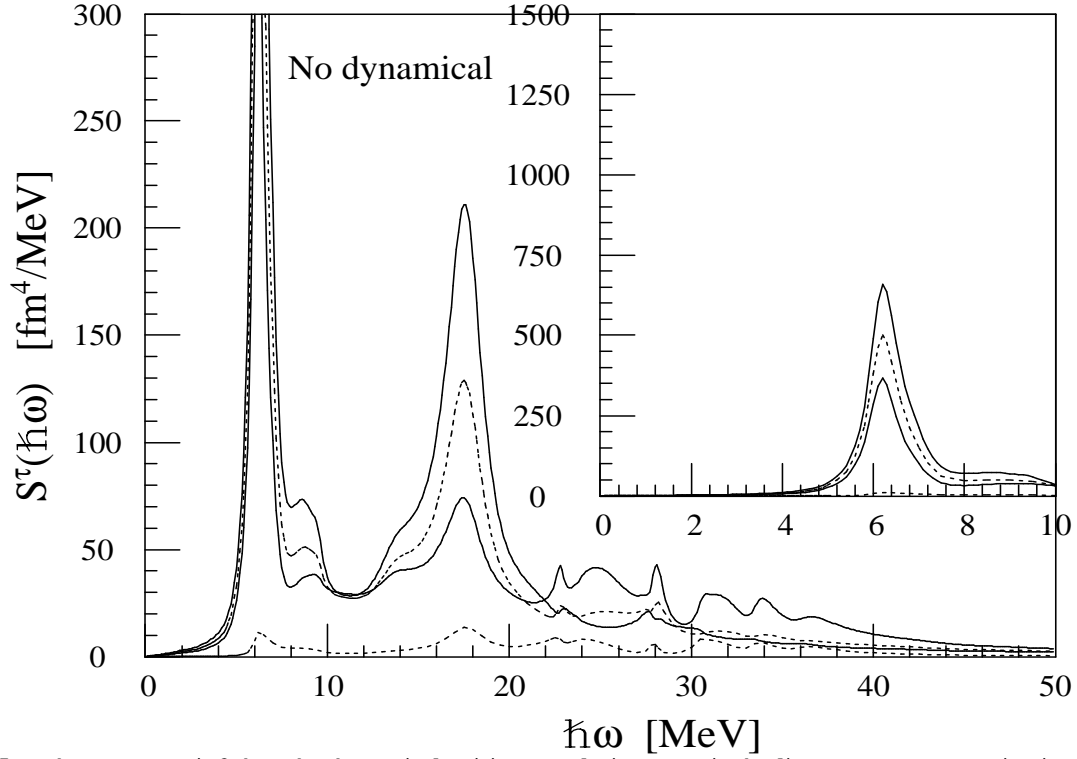


FIG. 5. The same as Fig. 2, but the dynamical pairing correlation effect in the linear response equation is neglected. Namely the density-dependent pairing is taken into account only in the static HFB mean-field.

There are two kinds of mechanisms in the pairing effects on the collective excitations. The first is a static effect. Since the static pair potential $v(r)$ in the HFB mean-field influences strongly the quasiparticle excitations, it hence affects the collective excitations. The second is dynamical. It is a correlation effect that is caused by the residual pairing interaction entering in the linear response equation (58). This arises because the collective excitations in the paired system induce not only the fluctuation in the density but also the fluctuations in the pair densities \tilde{n}_+ and \tilde{n}_- , for which correlation is brought by the residual pairing interaction (see, Eq.(58)). To quantify this dynamical pairing correlation effect, we show in Fig. 5 a calculation in which the pairing interaction is neglected in the linear response equation (58), but included in the static HFB mean-field. Comparison with Fig. 2 shows that the dynamical pairing correlation has a sizable effect to lower the excitation energy of the low-lying neutron mode by about 1 MeV. (One may also note that the width of the low-lying mode increases slightly in this calculation.) Performing a calculation where the particle-hole interaction is neglected, we find that the low-lying neutron mode is produced also by the pairing interaction alone, although the particle-hole residual interaction together is essential to make the collectivity large. If we used the conventional monopole pairing force (the seniority force) instead of the zero-range pairing force, the dynamical pairing correlation effect would be missed. The dynamical effect is rather related to effects of the quadrupole pairing that has been discussed in connection with the low-lying quadrupole mode in stable nuclei.

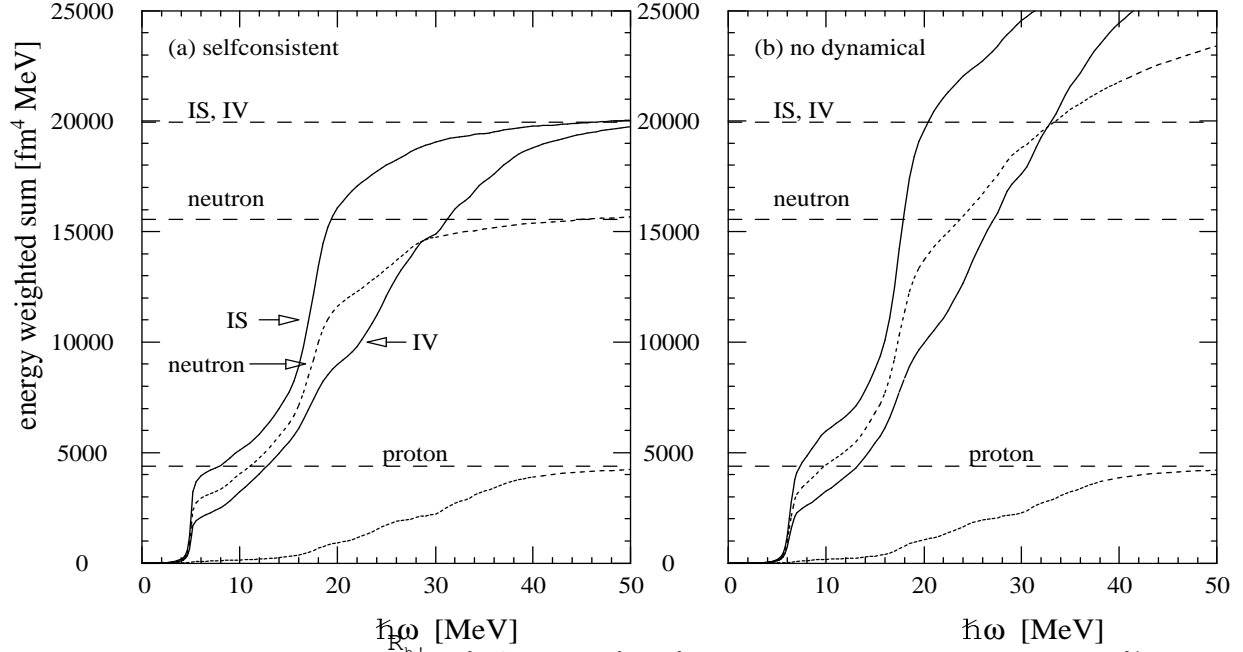


FIG. 6. (a) Energy weighted sum $\sum_0^{R_{h!}} h! S^{IS;IV;n;p}(h!)hd!^0$ of the quadrupole strength functions in ^{24}O , shown in Fig. 2. Here the density-dependent pairing is taken into account selfconsistently both in the static HFB mean-field and in the linear response equation. The dashed horizontal lines show the sum rule values for isoscalar (the same for isovector) transitions, and those for the neutron and the proton transition strengths. (b) The same as (a), but the dynamical pairing effect is neglected (cf. Fig. 5). Namely the pairing is taken into account only in the static HFB mean-field.

One of the most important characteristics of the present theory is that the energy weighted sum rule

$$\sum_0^{R_1} h! S^{IS;IV}(h!)hd! = \frac{25h^2}{4m} N r_n^2 + Z r_p^2; \quad (62a)$$

$$\sum_0^{R_1} h! S^{n;p}(h!)hd! = \frac{25h^2}{4m} N r_n^2; \frac{25h^2}{4m} Z r_p^2; \quad (62b)$$

is satisfied very accurately. The sum rule should hold since the adopted residual interactions (both the particle-particle pairing force v_{pair} and the particle-hole interaction v_{ph}) keep the Galilei invariance [42], i.e., they commute with the quadrupole operator $r^2 Y_{2M}(\hat{r})$. This is demonstrated in Fig. 6 (a) that shows the calculated energy weighted sum $\sum_0^{R_{h!}} h! S^{IS;IV;n;p}(h!)hd!^0$ ($= IS;IV;n;p$) as a function of the energy boundary $h!$. We stress here that the selfconsistent treatment of the pairing both in the static HFB and in the dynamical linear response is crucial to satisfy the sum rule. This is shown in Fig. 6 (b). This plots the energy weighted sum obtained in a truncated calculation in which the residual pairing interaction is neglected in the linear response equations (cf. the corresponding strength function is shown in Fig. 5). In this calculation, the sum rule Eq. (62) is strongly violated by about 50% for neutrons. The violation is significant especially in the high lying region ($E > 10$ MeV), as the strength in this region (shown in Fig. 5) apparently overestimates that of the full calculation (Fig. 2). The violation originates from the inconsistent treatment of the pairing interaction in the calculation of Figs. 5 and 6 (b), where the pairing correlation is included only in the HFB static mean-field, but neglected in the linear response equation. One can understand this by noting that the static pair potential (r) violates the Galilei invariance, i.e., it does not commute with the density operator. By taking into account selfconsistently the pairing interaction in the linear response equation, the Galilei invariance of the original pairing interaction is recovered, and the sum-rule is satisfied. This corresponds to a previous result [47] showing that the sum rule violated by the monopole pairing potential can be remedied by including the selfconsistent quadrupole pairing interaction that recovers the Galilei invariance. The selfconsistent treatment of the pairing is important especially in the case of the density-dependent pairing force and in nuclear drip-lines since in such cases the pairing potential (r) in the surface region becomes relatively large.

We have also checked that the selfconsistency in the pairing is fulfilled in the present calculation, by investigating the Nambu-Goldstone mode in the response functions for the monopole pair operators $P_0^Y =$

R
 $\int dr P^Y(r)$ and $P_0 = (P_0^Y)^Y$. When the HFB static pairing potential $V(r)$ is not zero, the pairing rotational mode that has zero excitation energy should emerge as a Nam bu-Goldstone mode associated with the nucleon number conservation of the Hamiltonian, or in other words the invariance with respect to the gauge rotation $e^{i\hat{N}\phi}$ [$\hat{N} = \int dr \rho(r)$ ($\rho(r)$ being the neutron or proton number operator)]. The monopole response calculated for ^{24}O exhibits the pairing rotational mode at the excitation energy very close to zero. It is found that we can move the energy of the pairing rotational mode exactly at zero energy just by modifying finely the pairing force strength V_0 within 1%. We also checked that the calculated monopole strength function for the nucleon number operators \hat{N} carries no spurious strengths. This is again achieved by including selfconsistently the dynamical pairing correlation in the linear response equation.

V. CONCLUSIONS

We have formulated a new continuum linear response theory on the basis of the Hartree-Fock-Bogoliubov formalism in the coordinate space representation. This enables us to describe the pairing correlation in nuclei near drip-lines in a selfconsistent way both in the static ground state and in the dynamical collective responses. The formalism is able to include effects of the one-particle and the two-particle continuum states on the collective excitations.

We have described the quadrupole response in the drip-line nucleus ^{24}O with use of the density-dependent zero-range interactions. The strength functions for the quadrupole transition moments are obtained up to the giant resonance region. A low-lying mode which has significant neutron collectivity and is embedded in the neutron continuum states is obtained. We have analyzed in detail pairing effects important for the low-lying neutron mode. It is found that the low-lying neutron mode is sensitive to the density-dependence of the pairing correlation especially near the drip-line. The collective excitations in paired systems induce fluctuations not only in the normal density but also in the pair densities. The residual part of the pairing interaction causes dynamical correlation effects on the responses through the pair density fluctuations. The present theory describes selfconsistently both the static pairing effect caused by the HFB pair potential and the dynamical pairing correlation in the linear responses. The energy weighted sum rule is satisfied very accurately. This is because the selfconsistent treatment of the pairing restores the Galilei invariance, which would be violated if the HFB pair potential alone was included.

ACKNOWLEDGMENTS

The author thanks K. Matsuyanagi for valuable comments and discussions.

-
- [1] P. Ring and P. Schuck, *The Nuclear Many-Body Problem*, Springer-Verlag, Berlin, 1980.
 - [2] I. Hamamoto, H. Sagawa, and X.Z. Zhang, *Phys. Rev. C* 53 (1996), 765; *C* 55 (1997), 2361; *C* 56 (1997), 3121; *C* 57 (1998), R1064;
 I. Hamamoto, H. Sagawa, and X.Z. Zhang, *Nucl. Phys. A* 626 (1997), 669; *A* 648 (1999), 203.
 - [3] S.A. Fayans, *Phys. Lett. B* 267 (1991), 443.
 - [4] F. Ghienetti, G. Colo, E. Vigezzi, P.F. Bortignon, and R.A. Broglia, *Phys. Rev. C* 54 (1996), R2143.
 - [5] S. Shlomo and G. Bertsch, *Nucl. Phys. A* 243 (1975), 507.
 - [6] G.F. Bertsch and S.F. Tsai, *Phys. Rep.* 18 (1975), 125.
 - [7] J.Dobaczewski, H. Flocard, and J. Treiner, *Nucl. Phys. A* 422 (1984) 103.
 - [8] J.Dobaczewski, W. Nazarewicz, T.R. Werner, J.F. Berger, C.R. Chinn, and J. Dedeckere, *Phys. Rev. C* 53 (1996) 2809.
 - [9] G.F. Bertsch and H. Esbensen, *Ann. Phys.* 209 (1991) 327.
 - [10] R. Smolanczuk and J.Dobaczewski, *Phys. Rev. C* 48 (1993) R2166.
 - [11] J.Dobaczewski, I. Hamamoto, W. Nazarewicz, and J.A. Sheikh, *Phys. Rev. Lett.* 72 (1994), 981.
 - [12] K. Bennaceur, J.Dobaczewski, and M. Ploszajczak, *Phys. Rev. C* 60, (1999), 034308.
 - [13] S.Mizutori, J.Dobaczewski, G.A. Lalazissis, W. Nazarewicz, and P.-G. Reinhard, *Phys. Rev. C* 61 (2000), 044326.
 - [14] J.Dobaczewski, W. Nazarewicz, and P.-G. Reinhard, preprint nucl-th/0103001.

- [15] S.V. Siminov, S.V. Tolbokonnikov, and S.A. Fayans, *Sov. J. Nucl. Phys.* 48 (1988), 995.
- [16] S.A. Fayans, S.V. Tolbokonnikov, E.L. Trykov, and D. Zawischa, *Phys. Lett. B* 338 (1994), 1.
- [17] S.A. Fayans, S.V. Tolbokonnikov, E.L. Trykov, and D. Zawischa, *Nucl. Phys. A* 676 (2000), 49.
- [18] J. Terasaki, P.-H. Heenen, H. Flocard, and P. Bonche, *Nucl. Phys. A* 600 (1996), 371.
- [19] J. Terasaki, H. Flocard, P.-H. Heenen, and P. Bonche, *Nucl. Phys. A* 621 (1997), 706.
- [20] M.V. Stoitsov, W. Nazarewicz, and S. Pittel, *Phys. Rev. C* 58 (1998), 2092.
- [21] N. Tajima, in: *Proc. Int. Symp. on Models and Theories of the Nuclear Mass*, Wako, Japan, July 19–23, 1999, *Riken Review* 26 (2000) 87.
- [22] M. Yamagami, K. Matsuyanagi, and M. Matsuo, preprint nucl-th/0010087, to appear in *Nucl. Phys. A*
- [23] J. Meng and P. Ring, *Phys. Rev. Lett.* 77 (1996), 3963; 80 (1998), 460.
- [24] W. Poschl, D. Vretenar, G.A. Lalazisis, and P. Ring, *Phys. Rev. Lett.* 79 (1997), 3841.
- [25] G.A. Lalazisis, D. Vretenar, W. Poschl, and P. Ring, *Nucl. Phys. A* 632 (1998), 363.
- [26] A.P. Platonov and E.E. Saperstein, *Nucl. Phys. A* 486 (1988), 63.
- [27] I.N. Borzov, S.A. Fayans, E. Kromer, and D. Zawischa, *Z. Phys. A* 355 (1996), 117.
- [28] S. Kamerdzhiev, R.J. Liotta, E. Litvinova, and V. Tselyaev, *Phys. Rev. C* 58 (1998), 172.
- [29] K. Hagino and H. Sagawa, preprint nucl-th/0102042.
- [30] J. Engel, M. Bender, J. Dobaczewski, W. Nazarewicz, and R. Summan, *Phys. Rev. C* 60 (1999), 014302.
- [31] E. Khan and Nguyen Van Giai, *Phys. Lett. B* 472 (2000), 253.
- [32] E. Khan, Y. Blumefeld, Nguyen Van Giai, T. Suomijarvi, N. Alamanos, F. Auger, G. Colb, N. Frascaria, A. Gillibert, T. Glesmacher, M. Godewin, K.W. Kemper, V. Lapoux, I. Lhenry, F. Morechal, D.J. Morrissey, A. Mumarra, N.A. Orr, S. Ottini-Hustache, P. Piattelli, E.C. Pollacco, P. Roussel-Chomaz, J.C. Royonette, D. Santonocito, J.E. Sauvestre, J.A. Scarpaci, C. Volpe, *Phys. Lett. B* 490 (2000), 45.
- [33] G. Colb and P.F. Bortignon, preprint nucl-th/0104009.
- [34] J.-P. Blaizot and G. Ripka, *Quantum Theory of Finite Systems* (The MIT Press, 1986).
- [35] S.T. Belyaev, A.V. Siminov, S.V. Tolbokonnikov, and S.A. Fayans, *Sov. J. Nucl. Phys.* 45 (1987), 783.
- [36] A.L. Fetter and J.D. Walecka, *Quantum Theory of Many-Particle Systems* (McGraw-Hill, 1971).
- [37] J. Terasaki, P.-H. Heenen, P. Bonche, J. Dobaczewski, and H. Flocard, *Nucl. Phys. A* 593 (1995), 1.
- [38] T. Duguet, P. Bonche, and P.-H. Heenen, *Nucl. Phys. A* 679 (2001), 427.
- [39] J. Blomqvist and S. Wahlborn, *Arkiv Fysik* 16 (1959), 545.
- [40] A. Bohr and B.R. Motelson, *Nuclear Structure. vol. I* (Benjamin, 1969).
- [41] M. Bender, K. Rutz, P.-G. Reinhard, and J.A. Maruhn, *Euro. Phys. J. A* 8 (2000), 59.
- [42] A. Bohr and B.R. Motelson, *Nuclear Structure. vol. II* (Benjamin, 1975).
- [43] S. Ramann, C.H. Maloney, W.T. Miller, C.W. Nestor, Jr., and P.H. Stelson, *Atom. Dat. Nucl. Dat. Tabl.* 36 (1987), 1.
- [44] J.K. Jewell, L.A. Riley, P.D. Cottle, K.W. Kemper, T. Glesmacher, R.W. Ibbotson, H. Scheit, M. Chromik, Y. Blumefeld, S.E. Hirsbruch, F. Morechal, T. Suomijarvi, *Phys. Lett. B* 454 (1999), 181.
- [45] P.G. Thirolf, B.V. Pritychenko, B.A. Brown, P.D. Cottle, M. Chromik, T. Glesmacher, G. Hackman, R.W. Ibbotson, K.W. Kemper, T. Otsuka, L.A. Riley, H. Scheit, *Phys. Lett. B* 485 (2000), 16.
- [46] F. Azaiez, *Phys. Scr. T* 88 (2000), 118.
M. Bellec, M.-J. Lopez-Jimenez, M. Stanoiu, F. Azaiez, M.-G. Saint-Laurent, O. Sorlin, N.L. Achouri, J.-C. Angélique, C. Bourgeois, C. Borcea, J.-M. Daugas, C. Donzaud, F. De Oliveira-Santos, J. Duprat, S. Gearty, D. Guillemaud-Mueller, S. Leenhardt, M. Lewitowicz, Yu.-E. Penionzhkevich, and Yu. Sobolev, *Nucl. Phys. A* 682 (2001) 136c.
- [47] T. Kubo, H. Sakamoto, T. Kamatori, and T. Kishimoto, *Phys. Rev. C* 54 (1996), 2331.